ILASS–Europe 2022, 31th Conference on Liquid Atomization and Spray Systems, 6-8 September 2022, Virtual, Israel

Investigating the Atomizer Performance within Aluminium Melt Atomization

Dilyan Kamenov*[1], Lydia Achelis[1], Volker Uhlenwinkel[2], Udo Fritsching[1,2]
[1]Particles and Process Engineering, University of Bremen, Bremen, Germany
[2]Leibniz Institute for Materials Engineering IWT, Bremen, Germany
*Corresponding author: d.kamenov@iwt.uni-bremen.de

Abstract
Investigation of the aluminium alloy melt (AlSi10Mg) atomization with a pressure gas atomizer (PGA), combining a pressure swirl liquid nozzle and a concentric gas nozzle, is done. The influence of the atomizer geometry and process parameters and the influence of the flow conditions is investigated. The performance of the atomizer is being evaluated by the powder size distribution (sauter mean diameter (SMD) and width of the size distribution (span)) as measured by means of laser diffraction spectrometry. In order to evaluate the performance of the atomizer design a comparison of the powders from conventional close coupled atomizer (CCA) with the novel atomizer design is made.

Keywords
atomization, pressure-swirl atomizer, airblast atomizer, metal atomization, aluminium

Introduction

The worldwide demand for high quality metal powders is steadily rising for instance due to the rapid emergence of additive manufacturing. In metal powder production the state-of-the-art atomizer is the close-coupled design. It consists of a circular plain orifice outlet for the melt feed surrounded by a ring slit gas nozzle which is mounted closely above on the same axis. The process involves the formation of a melt plume in the vicinity of the outlet through upward recirculation and radial pressure gradients [1]. The atomizing velocities within the melt plume are highly heterogenous and significantly lower than the gas velocities. Furthermore, the gas to liquid ratio in the atomization region is also found to be subject to fluctuations. These effects lead to kinetic energy transfer efficiencies of <0.02% [2] and broad particle size distributions [3].
Thus a novel atomization technique was designed, which showed promising results during atomization of water compared to a conventional close-coupled atomizer (CCA), i.e. lower SMD at lower gas to liquid ratios (GLR) and generally narrower particle size distributions [4]. Some previous studies of this particular atomizer were carried out with tin and tin copper alloys [5, 6], but not with aluminium based alloys, which exhibit higher surface tensions at their respective melting points [7, 8]. The present contribution ties in with an assessment of the performance within argon atomization of AlSi10Mg.

Material and Methods

A schematic representation of the PGA and CCA atomizer designs and their respective flow conditions is given in **Figure 1**.

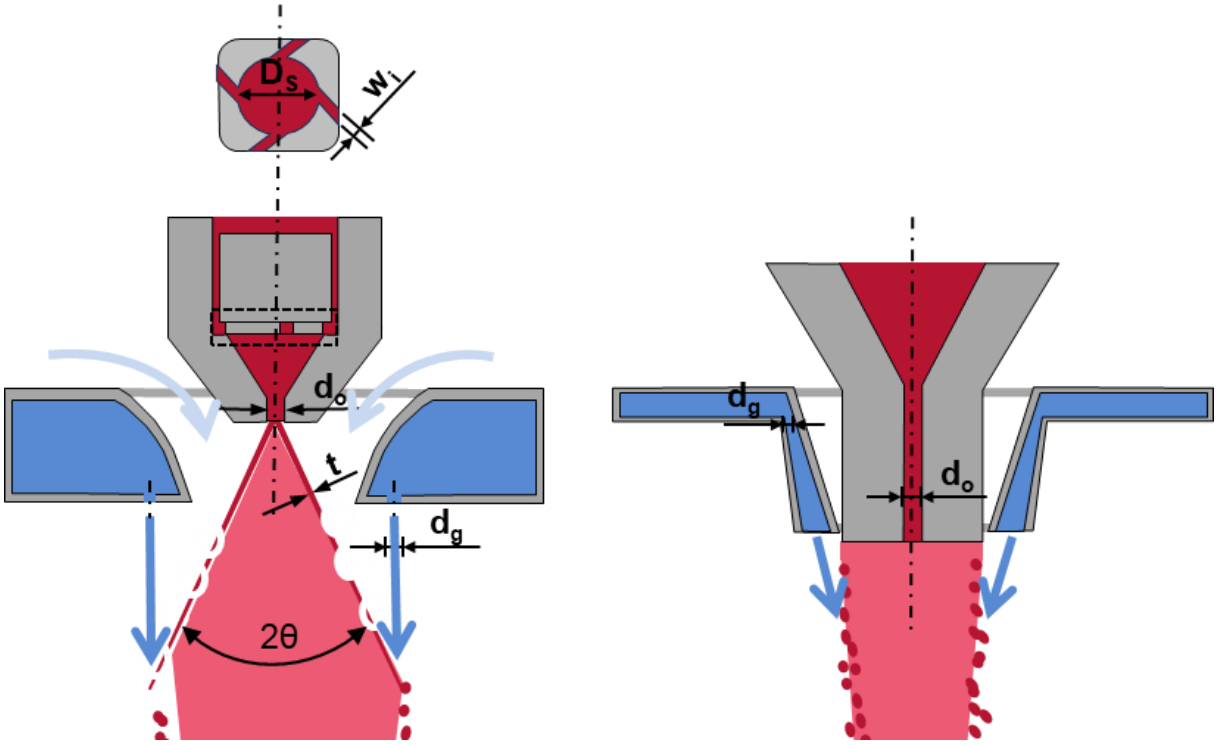

Figure 1. Schematic representation of the PGA (left) and CCA (right)

In order to induce the swirl of the liquid within the pressure swirl nozzle, it is being guided through a number of square tangential inlets (n_i) with the width of w_i into a swirl chamber with a diameter of D_s. Four inlets showed the best results when atomizing water, i.e. lower dependency of SMD on GLR. Furthermore, the liquid is being accelerated in the axial direction due to the narrowing of the nozzle towards the outlet. Three orifice diameters d_o, namely 1.0, 1.5 and 2.0 mm were examined. The centrifugal forces result in the liquid exiting the nozzle in the form of a hollow cone with a lamella thickness t of a few hundred micrometres, which is crucial for producing fine droplets as it is proportional to droplet size. Another important parameter is the hollow cone half-angle θ. Larger θ shift the gas impact region closer to the gas nozzle outlets, thus improving the momentum exchange between both phases. Following equations can be used to calculate lamella thickness t [9] and cone angle θ [10] respectively for this specific nozzle:

$$t^2 = \frac{1560\dot{m}_L\mu_L}{\rho_L d_o \Delta p_L}\frac{1+(d_o-2t)^2/d_o^2}{(1-\frac{(d_o-2t)^2}{d_o^2})^2}, \quad (1)$$

$$2\theta = 6\left(\frac{n_i\cdot(w_i)^2}{D_s\cdot d_o}\right)^{-0.15}\left(\frac{\Delta p_L d_o^2 \rho_L}{\mu_L^2}\right)^{0.11}, \quad (2)$$

where $\dot{m}_L$ is the melt mass flow rate, ρ_L and μ_L are the melt density and dynamic viscosity respectively and Δp_L is the pressure acting on the melt.

To complement the primary atomization mode, because of instabilities within the coherent liquid itself, an annular gas nozzle mounted underneath the pressure swirl nozzle induces secondary atomization by impinging a gas stream on the liquid phase.

The gas nozzle consists of 20 circular orifices with a diameter d_g = 1.1 mm (total area $1.90 \cdot 10^{-5}$ m²) concentrically arranged on a ring with a diameter of 22 mm.
It is fixed below the pressure swirl nozzle to allow for gas to be entrained (see light blue arrows in **Figure 1**, left) by the expanding gas jets and reduce pressure gradients and recirculation near the melt exit, which might influence process stability.
The chosen CCA configuration (**Figure 1**, right) consists of a circular plain orifice d_o = 2.0 mm to ensure the free discharge of melt. In a coaxial design the goal is to maximise the relative velocity between both phases and thus only a small overpressure is exerted on the melt.
The ring slit gas nozzle is convergent-divergent and the width at the narrowest point is 0.8 mm (total area $4.62 \cdot 10^{-5}$ m²). In general it can be observed that the SMD decreases with an increase in GLR [11].
In order to quantify the width of the powder size distributions, the *span* can be calculated as follows:

$$span = (d_{90} - d_{10})/d_{50}, \quad (3)$$

with the characteristic diameters d_i such that i% of the total volume particle distribution is made up of particles smaller than the respective diameter.
Table 1 shows an overview of the experiments with both nozzle designs.

Table 1 - Overview of the experiments with the CCA and PGA

Atomizer	[-]	CCA			PGA						
Exp. Nr.	[-]	78	79	80	88	91	93	94	97	102	107
Gas pressure	[Pa]	$14 \cdot 10^5$	$12 \cdot 10^5$	$10 \cdot 10^5$	$12 \cdot 10^5$	$12 \cdot 10^5$	$16 \cdot 10^5$	$20 \cdot 10^5$	$20 \cdot 10^5$	$20 \cdot 10^5$	$20 \cdot 10^5$ No entrainment
Melt pressure	[Pa]	$(30\text{-}50) \cdot 10^2$	$(30\text{-}50) \cdot 10^2$	$(30\text{-}50) \cdot 10^2$	$6 \cdot 10^5$	$7 \cdot 10^5$	$7 \cdot 10^5$	$7 \cdot 10^5$	$7 \cdot 10^5$	$7 \cdot 10^5$	$7 \cdot 10^5$
d_o	[mm]	2	2	2	2	2	2	2	1	1,5	1,5
Gas mass flow rate	[g/s]	150,40	129,20	108,70	57,42	57,42	71,64	91,08	91,08	91,08	102,78
Melt mass flow rate	[g/s]	16,74	17,62	18,22	52,63	59,10	59,51	50,37	21,68	37,16	37,09
GLR	[-]	8.94	7.33	5.97	1.09	0.97	1.20	1.81	4.20	2.45	2.77
SMD	[µm]	26.46	33.20	35.29	102.82	87.14	88.03	91.84	98.90	83.52	40.64
span	[-]	1.88	1.73	1.93	1.74	1.70	1.73	1.63	1.43	1.83	2.46

All experiments were carried out at an initial melt temperature of 1073 K, the atomizing gas employed was argon at ambient temperature. The gas pressure for the CCA experiments varied between 10 and $14 \cdot 10^5$ Pa, lower pressures are not feasible for producing fine metal powders with this atomizer design. The gas pressures employed with the PGA were chosen between 12 and $20 \cdot 10^5$ Pa.

The melt pressure in the CCA crucible was ramped up from 30 kPa at the beginning to 50 kPa at the end of the atomization run to counteract the decrease in metallostatic pressure as the melt volume in the crucible decreases and thus ensure a constant pressure on the melt.
A pressure swirl atomizer needs higher pressures to ensure a fully developed cone, hence the experiments were carried out a melt pressure of $7 \cdot 10^5$ Pa and one of the experiments was carried out at $6 \cdot 10^5$ Pa to show the influence of this parameter.
In order to investigate the influence of the entrainment flow on the atomization process in experiment 107 the gap between pressure swirl nozzle and gas nozzle was closed.
The powders produced with the CCA were sieved with a 200 µm sieve and the PGA powders with a 500 µm sieve. The purpose of the sieving is to remove non-spherical particles which result from large melt droplets colliding with the walls of the powder production tower and solidifying in the form of so-called splats. The maximum sieving residue of the CCA powders is 0.7% of the total powder mass and the maximum of the PGA powders is 8.9%, whereas the lowest value is 1.9%. These values can be used to estimate the maximum error in the measured SMD. A Mastersizer 2000 by Malvern Panalytical (wet dispersion unit with distilled water), which operates on the principle of laser diffraction, was employed to measure three samples of each powder three times and calculate the average SMD and span.

Results and Discussion

Figure 2 shows the influence of different parameters on the SMD as a function of GLR for both nozzle designs.

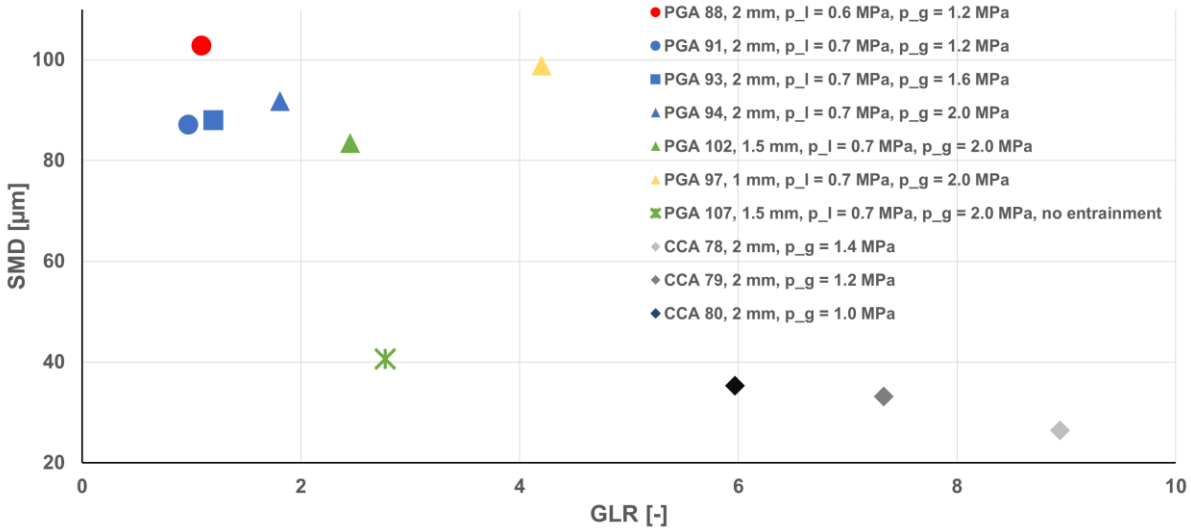

Figure 2. Influence of different parameters on SMD as a function of GLR for both nozzle designs

By looking at the circles it can be seen that an increase of melt pressure from 6 (red) to $7 \cdot 10^5$ Pa (blue) within the PGA leads to a decrease in SMD, even though the GLR also decreases as a result of the increased melt flow through the pressure swirl atomizer. This is a combination of two effects: an increase of hollow cone angle with an increase in melt pressure (see **Eq. 2**), which in turn improves momentum transfer between the melt and gas jets of the nozzle, and an increase in the instabilities in the lamella as a result of the increased pressure on the melt. According to **Eq. 1** the lamella thickness slightly decreases from 383 to 379 µm, which should have almost no effect in this case, but for higher pressure differences the effect would be stronger and have more impact on the atomization.

The hollow cone angle plays a very important role in this particular design, as can be seen by the blue symbols, which show the influence of the gas pressure on the SMD. The SMD increases even though the GLR increases since a higher manifold pressure increases the gas density at the orifice and thus the mass flow rate. Here, the potentially positive effect of an increased GLR is offset by an accompanying increase in entrainment mass flow rate between both nozzles, which is proportional to the manifold pressure. The momentum of the entrainment mass flow increases and pushes the hollow cone inwards, thus leading to smaller momentum transfer between the lamella and gas nozzle jets.
The cone angle and the interaction between lamella and entrainment flow are also particularly affected by the orifice diameter of the pressure swirl atomizer. The triangles show the influence of this geometrical parameter on the atomization result. A decrease of orifice diameter from 2.0 (blue) to 1.5 mm (green) leads to a decrease in SMD and then an increase by further reduction to 1.0 mm (yellow). The GLR is increasing because the melt flow rate decreases with a decrease in orifice diameter at otherwise identical geometrical and process parameters. In this case, **Eq. 1** predicts a decrease in lamella thickness from 363 to 315 and 251 µm, respectively. However, the hollow cone angle also decreases thus leading to a decreased momentum transfer between gas and melt. According to **Eq. 2** the difference in the cone angle between 2.0 and 1.5 mm is approximately 10% but the difference between 2.0 and 1.0 mm is ≈ 25%. The hollow cone is also influenced by the entrainment flow between the gas nozzle and the pressure swirl nozzle, which should be the same since the gas pressure is constant. **Figure 3** shows the hollow cone before the gas is turned on, on the top row and the hollow cone after the gas is turned on (bottom row). The difference in the undisturbed hollow cone angle is negligible for 2.0 and 1.5 mm, but for 1.0 mm it is significantly smaller.

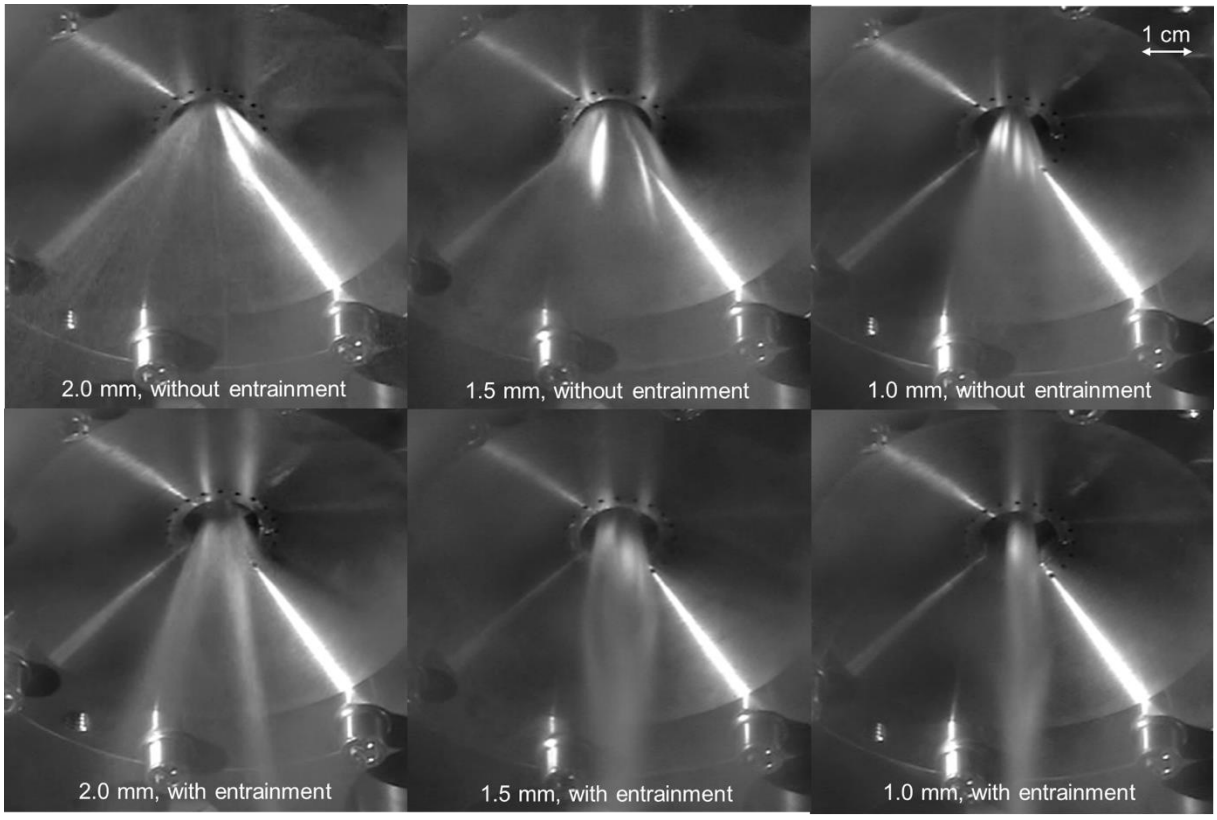

Figure 3. Hollow cone lamellas for 2.0, 1.5, and 1.0 mm orifice diameter at $7 \cdot 10^5$ Pa melt pressure without entrainment mass flow (top row) and with entrainment mass flow (bottom row)

Additionally, the momentum of the lamella decreases, since the melt mass flow decreases because of the smaller orifice even though the melt pressure and thus the potential velocity are the same. The lower momentum leads to a significant squeezing of the hollow cone by the entrainment flow, leading to the results seen in the bottom row. For the 2.0 and 1.5 mm orifices there is still a notable angle between the lamella and the jets of the nozzle, while both phases are basically flowing coaxially in the 1.0 mm configuration.
Because of the entrainment, experiment 107 (green cross) has been carried out at the same process and geometrical configuration as 102 (green triangle), but the gap allowing for entrainment was sealed. This measure significantly improved the SMD by a factor of two at a slightly higher GLR.
The CCA experiments (grey symbols) show a decrease in SMD with GLR as expected. In comparison with experiment 107 with the PGA the SMDs are 15 - 35% lower, but at the cost of a GLR that is higher by a factor of 2.15 - 3.25.
Figure 4 illustrates the influence of different parameters on the span for both nozzle designs. In general, the mean span of all PGA experiments (1.79) is lower than the mean span of all CCA powders (1.85). Thus, a narrower particle size distribution can be produced by the PGA.

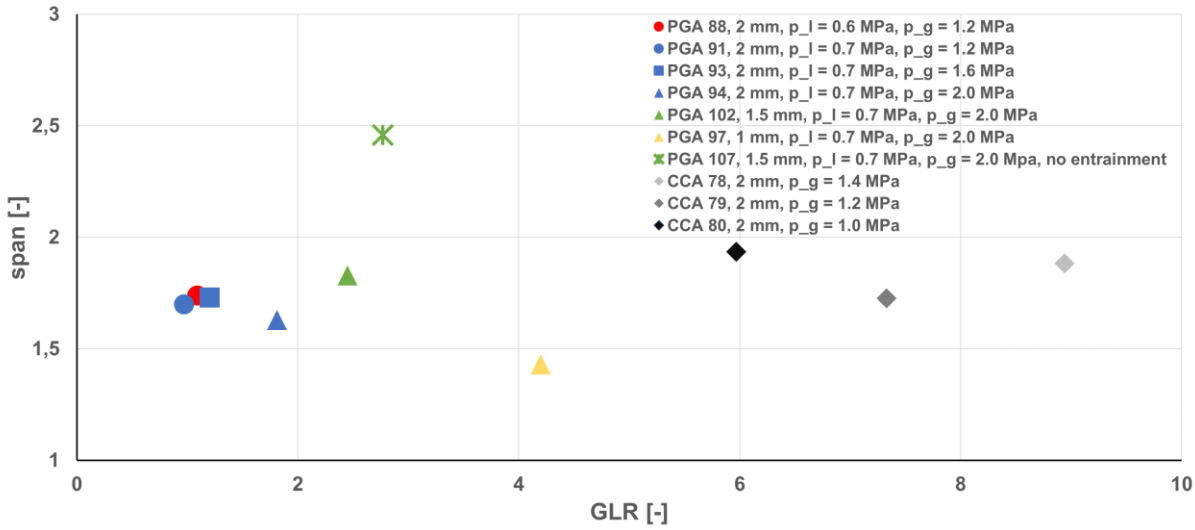

Figure 4. Influence of different parameters on span as a function of GLR for both nozzle designs

The PGA powders produced with the 1.0 mm orifice shows a very narrow distribution with a span of 1.43. The other significant result is the distinctly higher span of the experiment 107 at 2.46, which was carried out without entrainment.

Conclusions

A novel atomizer design (PGA) consisting of a combination of a pressure swirl liquid nozzle and a concentric discrete jet gas nozzle was investigated within aluminum atomization. The cone angle produced by the pressure swirl nozzle was identified as a major influence on atomization result, as it dictates the momentum transfer between melt stream and gas jets. It can be increased by increasing melt pressure, leading to smaller SMD, even though the GLR decreases as the melt mass flow increases. The momentum of the gas entrainment flow influences the cone angle to a large degree. An increase in manifold pressure in the gas nozzle increases the entrainment mass flow, thus squeezing the cone angle and increasing SMD, even though GLR increases. Furthermore, if the orifice diameter is reduced such that the momentum of the melt cone and its angle become too low to counteract the entrainment flow momentum sufficiently, the SMD increases. These findings are supported by the improvement in SMD achieved when entrainment is prevented, as the pressure swirl atomizer fluid dynamics are not disturbed allowing for maximum contact angle to the gas jets.

Compared to a close-coupled atomizer the finest PGA powder has an SMD just 15-35% larger at GLRs lower by a factor of 2.15-3.25. However, this particular powder has a significantly wider distribution with a span of 2.46 compared to the CCA powders (mean span of 1.85). The other PGA produced powders exhibit distributions with spans ranging from 1.43 to 1.83.
The next steps in the investigation of the novel atomizer design are to examine the reproducibility of the results, analyse the influences on the span in order to produce powders with a small SMD and a narrow distribution, as well as optimize the process parameters.

Acknowledgments
The project is funded by the German Federal Ministry for Economic Affairs and Energy (BMWi) within the “Zentrales Innovationsprogramm Mittelstand” (funding number: 16KN078702). The authors are grateful for the financial support and to the project partners Indutherm Gießtechnologie GmbH (Walzbachtal, Germany) and DHCAE Tools (Krefeld, Germany) for the collaboration.

Nomenclature

GLR	gas to liquid ratio [-]
CCA	close coupled atomizer
d_g	characteristic gas nozzle diameter [m]
D_s	swirl chamber diameter [m]
d_o	orifice diameter [m]
d_i	diameter such that i% of the total liquid volume is in droplets of smaller diameter [m]
n_i	number of inlets of the pressure swirl nozzle [-]
PGA	pressure gas atomizer
SMD	sauter mean diameter [m]
span	span of the droplet size distribution [-]
w_i	width of the square tangential inlet channel [m]
Δp_L	pressure difference [Pa]
θ	hollow cone half angle [°]
μ_L	liquid viscosity [kg·m^{-1}·s^{-1}]
ρ_L	liquid density [kg·m^{-3}]

References

1. Klar, E.F.J.W., *Atomization*, in *Metals Handbook*. 1984, American Society for Metals: Metals Park, OH.
2. Bigg, T.D. and A.M. Mullis, *Spatially Resolved Velocity Mapping of the Melt Plume During High-Pressure Gas Atomization of Liquid Metals.* Metallurgical and Materials Transactions B, 2020. **51**(5): p. 1973-1988.
3. Anderson, I.E. and R.L. Terpstra, *Progress toward gas atomization processing with increased uniformity and control.* Materials Science and Engineering: A, 2002. **326**(1): p. 101-109.
4. Kamenov, D., et al., *Investigating the performance of an airblast pressure swirl atomizer.* International Conference on Liquid Atomization and Spray Systems (ICLASS), 2021. **1**.
5. Lagutkin, S., et al., *Atomization process for metal powder.* Materials Science and Engineering A, 2004. **383**: p. 1-6.
6. Achelis, L., et al., *Spray angle and particle size in the pressure gas atomization of Tin and Tin-Copper alloys.* Proceedings of the World Powder Metallurgy Congress and Exhibition, World PM 2010, 2010. **1**.
7. Leitner, M., et al., *Thermophysical Properties of Liquid Aluminum.* Metallurgical and Materials Transactions A, 2017. **48**(6): p. 3036-3045.

8. Yuan, Z.F., et al., *Surface tension and its temperature coefficient of molten tin determined with the sessile drop method at different oxygen partial pressures.* J Colloid Interface Sci, 2002. **254**(2): p. 338-45.
9. Lefebvre, A.H. and V.G. McDonell, *Atomization and sprays*. Second Edition ed. 2017, Boca Raton: CRC Press.
10. N.K. Rizk and A.H. Lefebvre, *Prediction of Velocity Coefficient and Spray Cone Angle for Simplex Swirl Atomizers.* International Journal of Turbo and Jet Engines, 1987. **4**(1-2): p. 65-74.
11. Urionabarrenetxea, E., et al., *Experimental study of the influence of operational and geometric variables on the powders produced by close-coupled gas atomisation.* Materials & Design, 2021. **199**.